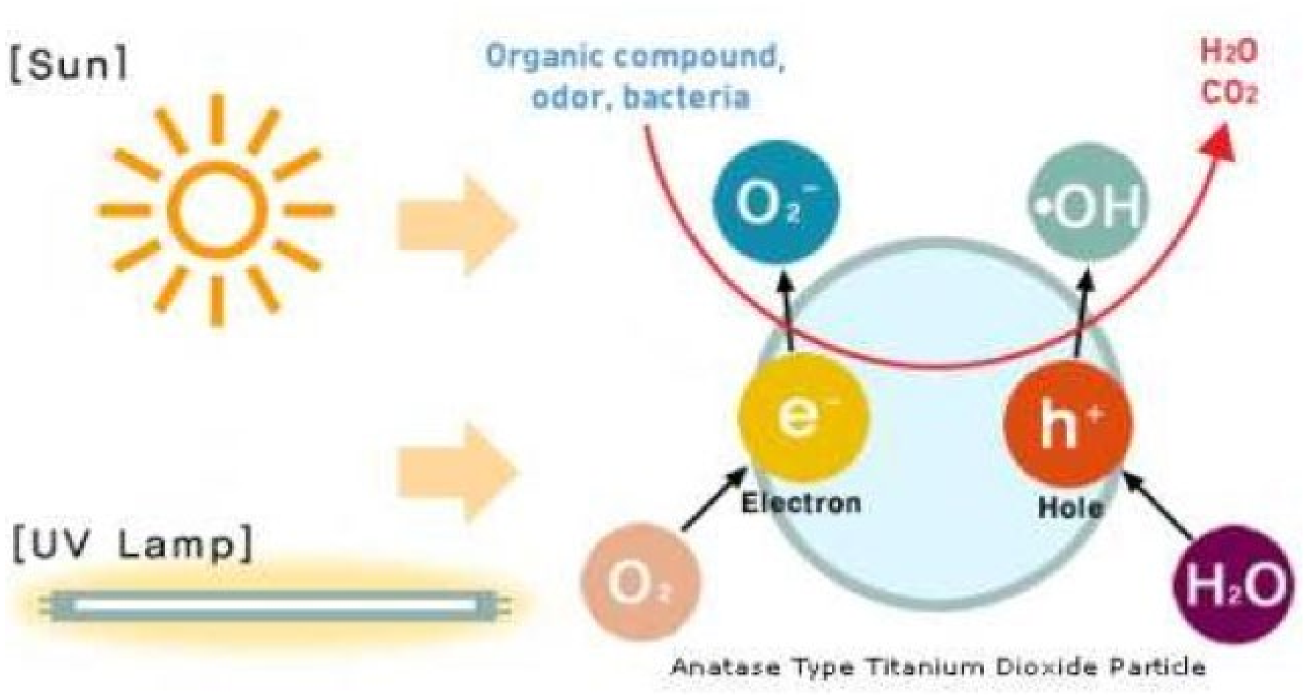

The role of Electron Spin Resonance in studying the photocatalytic mechanism of semiconductor oxides

Surface reactions

$H_2O_2 + e^- \rightarrow OH^\bullet + OH^-$

$O_2 + e^- \rightarrow O_2^{\bullet -}$

$O_2^{\bullet -}$ centers may further generate H_2O_2 [8,17,18]:

$O_2^{\bullet -} + H_2O \rightarrow HO_2^\bullet + OH^-$

$HO_2^\bullet + H_2O + e^- \rightarrow H_2O_2 + OH^-$

$H_2O_2 + O_2^{\bullet -} \rightarrow OH^\bullet + OH^- + O_2$

$$O^{2-} + h^+ + H^+ \rightarrow OH^\bullet \qquad (2)$$

O^- and $OH^\bullet$ species react with the organic substrates, generating organic radicals [11]:

$$O^-/OH^\bullet + PhOH \rightarrow O^{2-}/OH^- + PhO^\bullet + H^+ \qquad (3)$$

The ESR results allow to optimize the photocatalitic mechanism also based on the relations with:

the crystal structure (energy gap)
the crystal morphology and surface area
the presence of mixed oxides
the doping with transition metal ions
the hybridization with polymer membranes

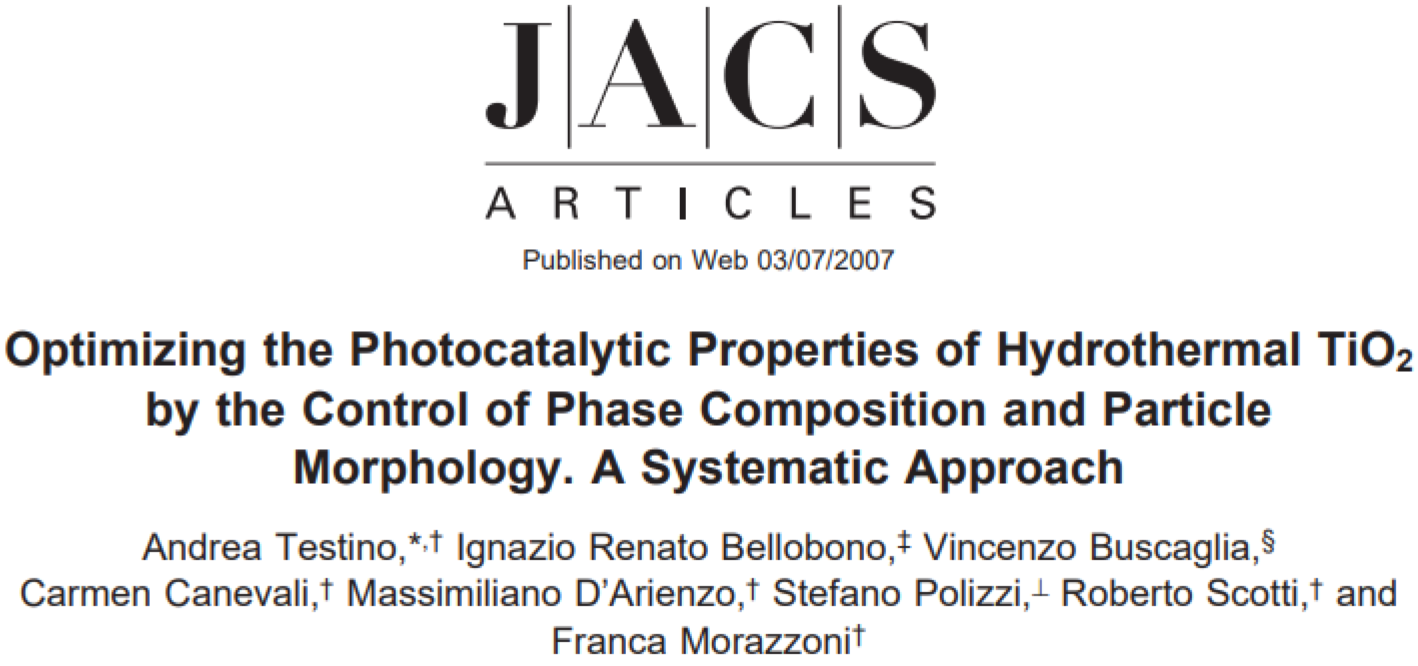

JACS
ARTICLES

Optimizing the Photocatalytic Properties of Hydrothermal TiO$_2$ by the Control of Phase Composition and Particle Morphology. A Systematic Approach

Andrea Testino,[*,†] Ignazio Renato Bellobono,[‡] Vincenzo Buscaglia,[§]
Carmen Canevali,[†] Massimiliano D'Arienzo,[†] Stefano Polizzi,[⊥] Roberto Scotti,[†] and
Franca Morazzoni[†]

This work was pioneer in our research but also a reference point of several following researches (more than 500 citations)

It has been there reported the selective preparation of TiO$_2$ as for the structure and the morphology, and for the first time they have been related to the catalytic activity

Rutile

Anatase

Mixed phase

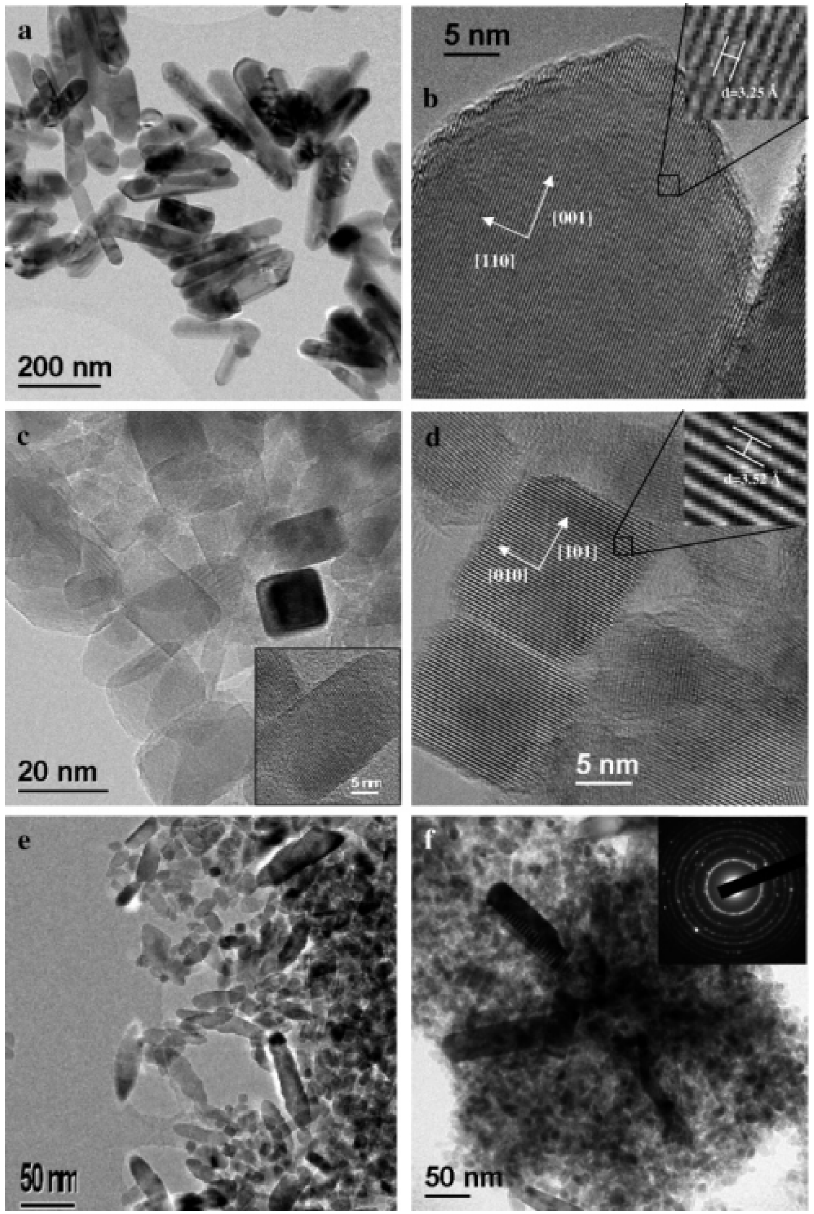

The morphology of the rutile crystals corresponds to faceted and elongated prismatic particles with an aspect ratio (length/width) of ~5.

The anatase particles have aspect ratios between 1 and 3. The particle size can be controlled by changing the experimental conditions and varies between 10 and 16 nm for anatase

The photocatalytic activity increases with increasing crystallite size. This suggests that the electron-hole pair recombination plays an important role during the photoprocess.

Charge recombination is apparently slower in well-faceted and big rutile particles, thus promoting a higher activity, despite the decrease of specific surface area.

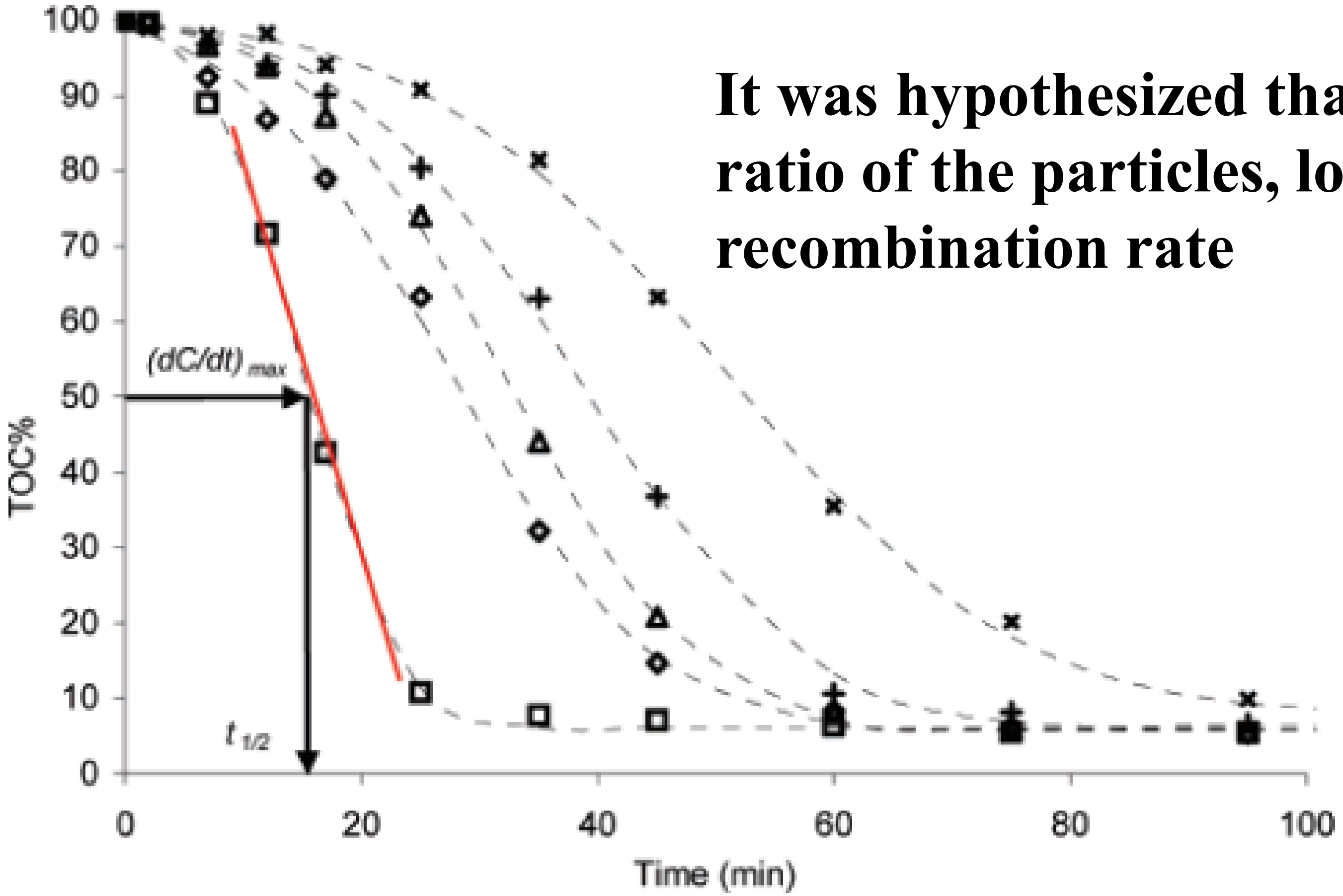

It was hypothesized that higher the aspect ratio of the particles, lower the electron-hole recombination rate

Figure 9. Mineralization curves of phenol (TOC %) of some representative samples (□: S371H; ◇: S18T; △: Degussa P25; +: S12T; ×: blank).

□ **S 371H mineralization curve of pure rutile**

ESR spectroscopy allows to detect the electrons and holes in the catalyst

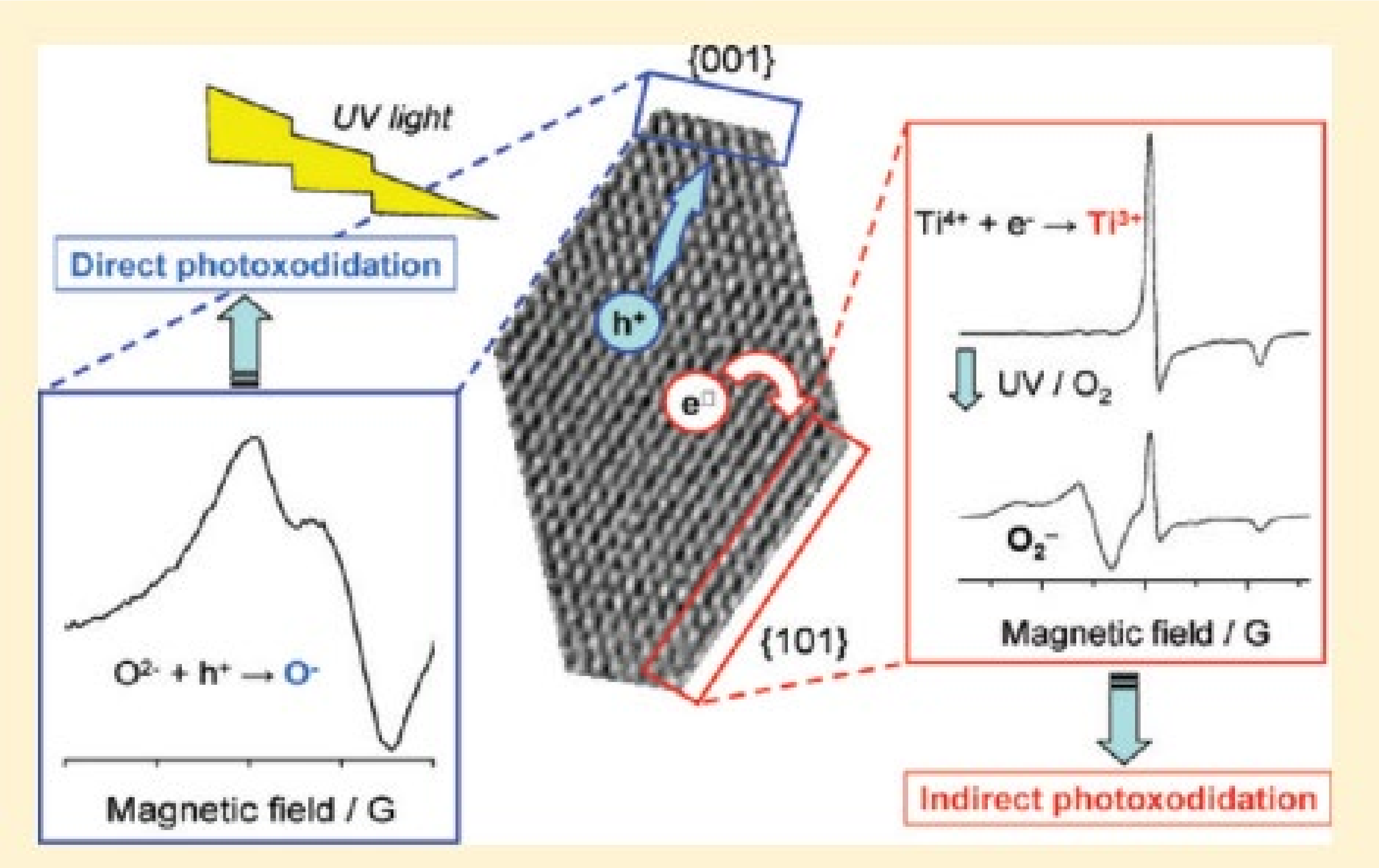

Fundamentals of ESR spectrocopy

A

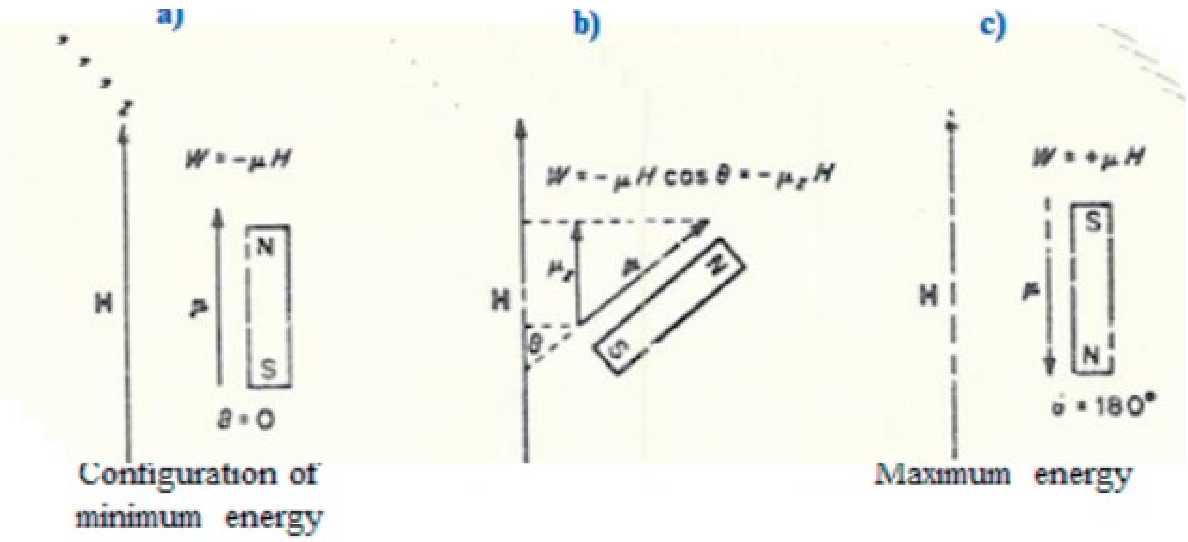

B

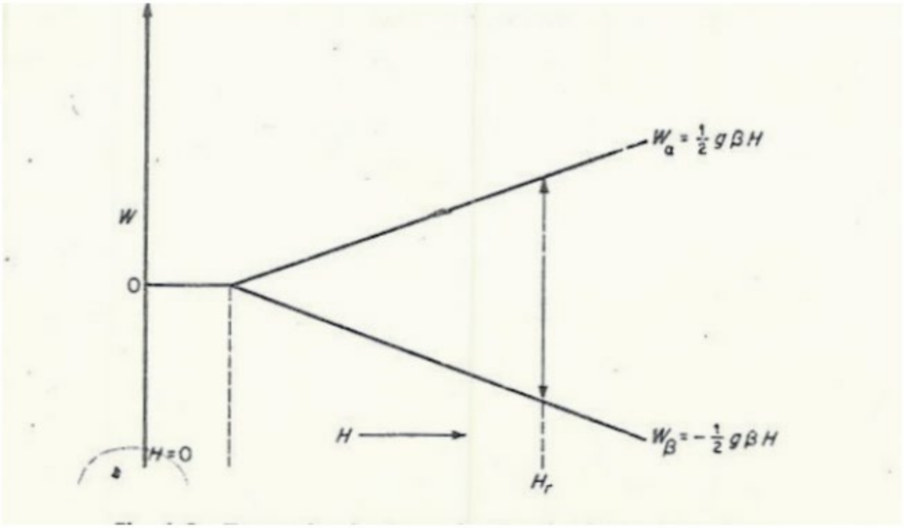

A) Energy interaction of one elecron in the magnetic field
B) Energy change induced by the magnetic field on one electron

g tensor dependence on the energy level trend of the paramagnetic centers

In the case of valence electrons

$$g_{ij} = g_e - 2\zeta \sum_{n \neq \psi_0} \frac{<\psi_0 | L_i | \psi_n ><\psi_n | L_j | \psi_0 >}{E_n^0 - E_0^0}$$

In the case of gap electrons

$$g_{ij} = g_e - 2\zeta \sum_{n \neq \psi_0} \frac{<\psi_0 | L_i | \psi_n ><\psi_n | L_j | \psi_0 >}{E_n^0 - E_0^0}$$

E_0 near C_B $g<g_e$ E_0 near V_B $g>g_e$

Paramagnetic species ESR active in TiO_2 semiconductor oxide

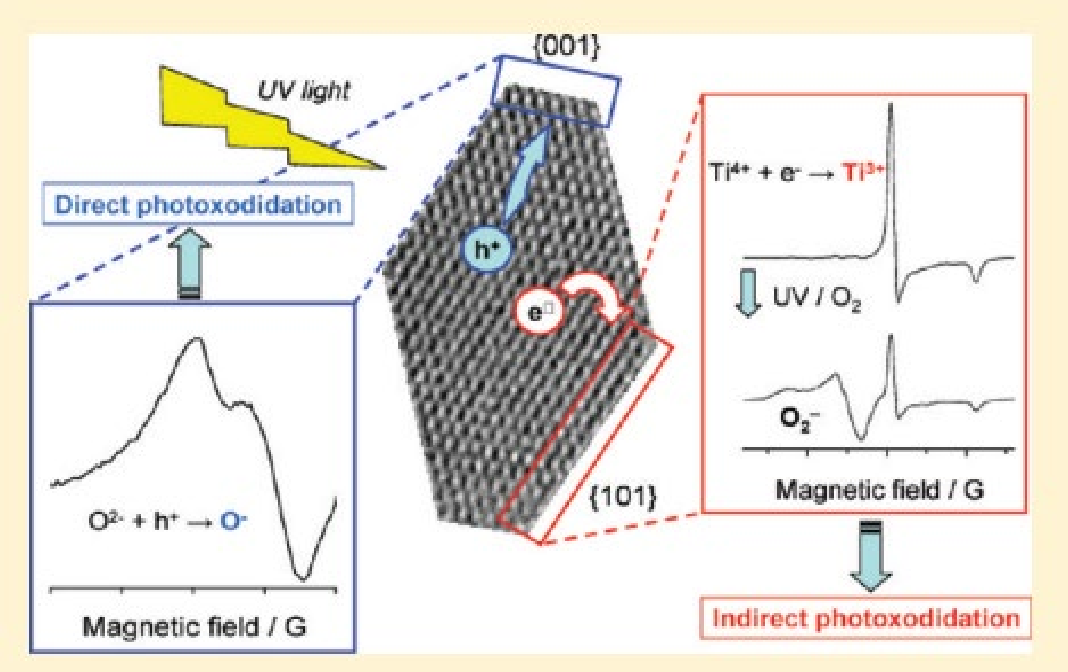

O^- O_2^- Ti^{3+}

Magnetic resonance prediction for O_2^-

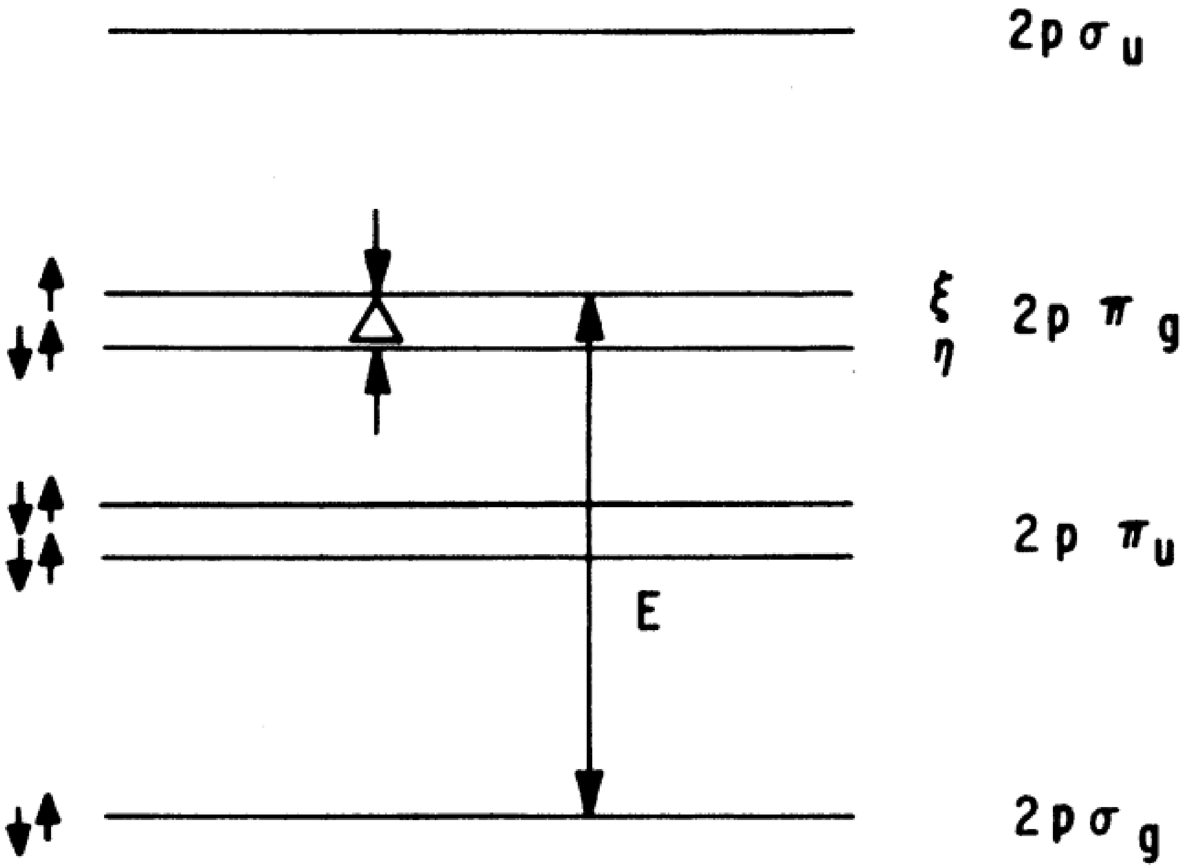

Energy level distribution in anisotropic O_2^-

$$g_\zeta = g_e + 2\left(\frac{\lambda^2}{\lambda^2+\Delta^2}\right)^{1/2} l,$$

$$g_\xi = g_e\left(\frac{\Delta^2}{\lambda^2+\Delta^2}\right)^{1/2} - \frac{\lambda}{E}\left[-\left(\frac{\lambda^2}{\lambda^2+\Delta^2}\right)^{1/2} - \frac{\Delta}{(\lambda^2+\Delta^2)^{1/2}} + 1\right]$$

$$g_\eta = g_e\left(\frac{\Delta^2}{\lambda^2+\Delta^2}\right)^{1/2} - \frac{\lambda}{E}\left[\left(\frac{\lambda^2}{\lambda^2+\Delta^2}\right)^{1/2} - \frac{\Delta}{(\lambda^2+\Delta^2)^{1/2}} - 1\right],$$

g tensor expressions in anisotropic O_2^-

Magnetic resonance prediction for anisotropic Ti^{3+}

$$d_{(x2-y2)} < d_{xz,yz} < d_{z^2}$$

If the unpaired electron lies in the d $x^2 - y^2$ orbital,

$$g_{zz} = 2 - 8\zeta/\Delta \quad \Delta = E(d_{x2-y2}) - E(d_{xy})$$
$$g_{xx,yy} = 2 - 2\zeta/\delta \quad \delta = E(d_{xz,yz}) - E(d_{x2-y2})$$

If the unpaired electron lies in the $d(z^2)$ energy of orbital,

$$g_{zz} = 2$$
$$g_{xx,yy} = 2 - 6\zeta/E(d_{xz,yz}) - E(d_{z^2})$$

If the unpaired electron lies in the (d_{xy}) orbital,

$$g_{zz} = 2 - 8\zeta/\Delta$$
$$g_{xx,yy} = 2 - 2\zeta/\delta$$

and for O^-

$g_{zz} = 2$ $g_{xx,yy} = 2.0023 - 2\zeta/\Delta E$ ΔE separation energy due to anisotropy

Detecting electrons and holes in TiO_2

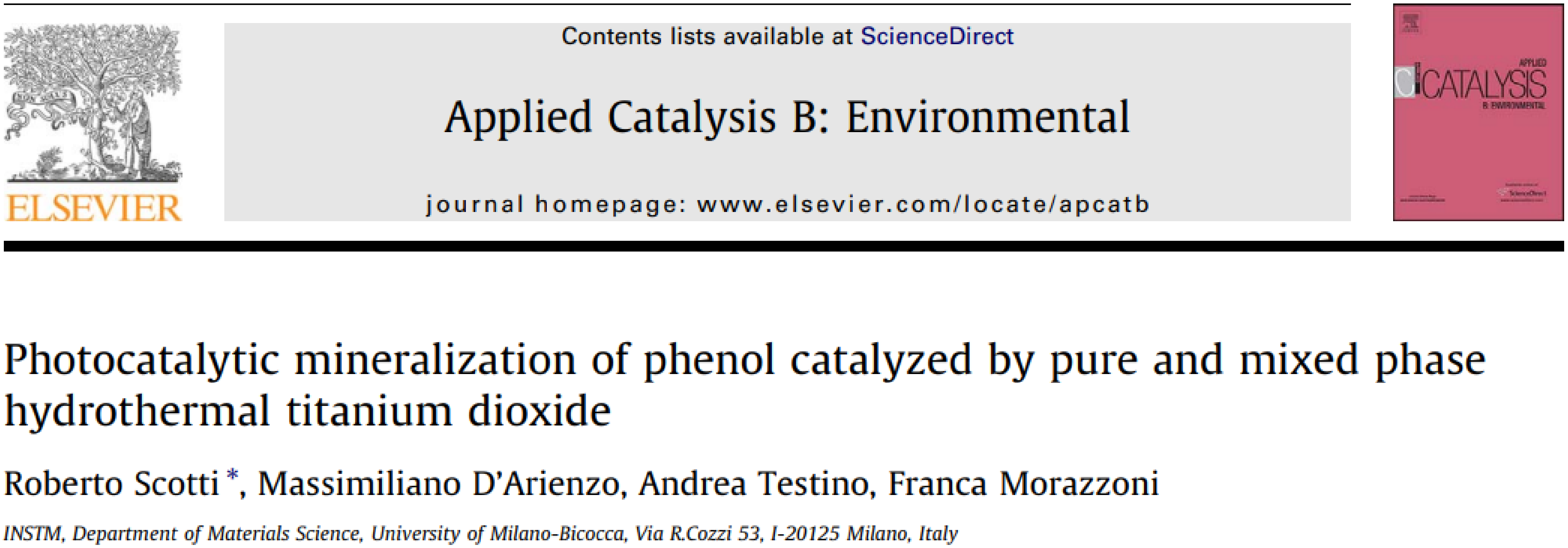

Contents lists available at ScienceDirect

Applied Catalysis B: Environmental

journal homepage: www.elsevier.com/locate/apcatb

Photocatalytic mineralization of phenol catalyzed by pure and mixed phase hydrothermal titanium dioxide

Roberto Scotti *, Massimiliano D'Arienzo, Andrea Testino, Franca Morazzoni

INSTM, Department of Materials Science, University of Milano-Bicocca, Via R.Cozzi 53, I-20125 Milano, Italy

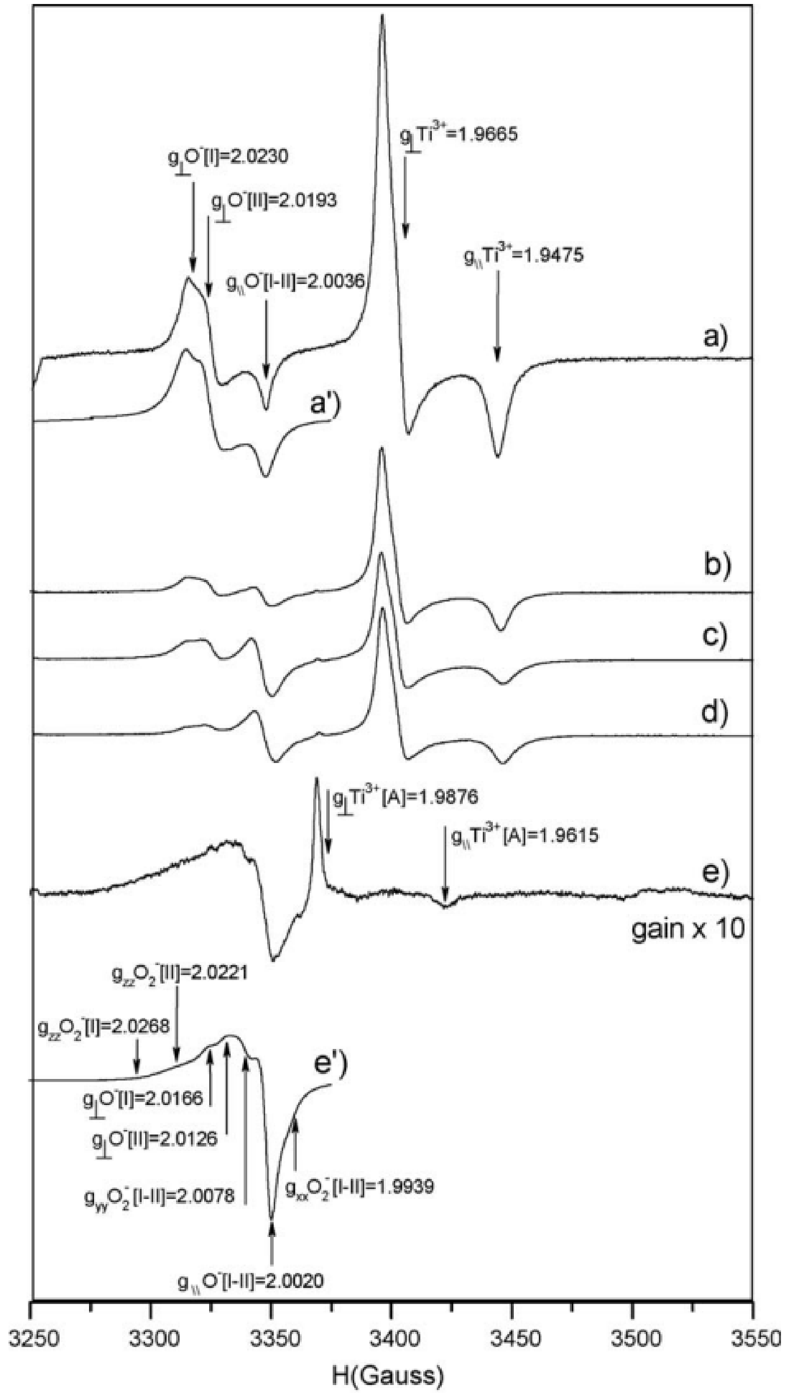

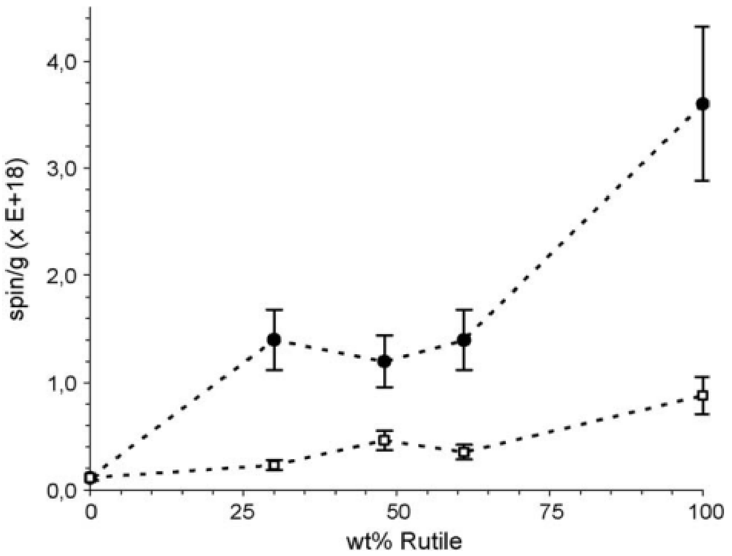

Amount of paramagnetic Ti^{3+} (■)and O^-(□)

a, b, c, d ESR spectra on samples, increasing the rutile amount

e ESR spectrum of pure anatase

Relevant suggestions based on photocatalytic and ESR parameters

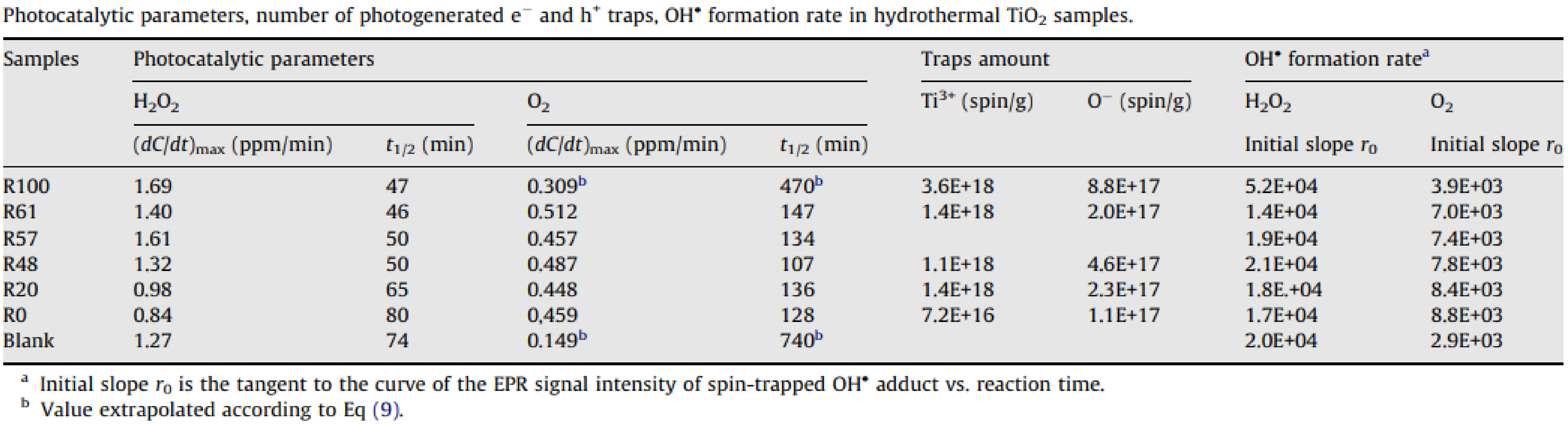

Photocatalytic parameters, number of photogenerated e^- and h^+ traps, $OH^\bullet$ formation rate in hydrothermal TiO_2 samples.

Samples	Photocatalytic parameters				Traps amount		$OH^\bullet$ formation rate[a]	
	H_2O_2		O_2		Ti^{3+} (spin/g)	O^- (spin/g)	H_2O_2	O_2
	$(dC/dt)_{max}$ (ppm/min)	$t_{1/2}$ (min)	$(dC/dt)_{max}$ (ppm/min)	$t_{1/2}$ (min)			Initial slope r_0	Initial slope r_0
R100	1.69	47	0.309[b]	470[b]	3.6E+18	8.8E+17	5.2E+04	3.9E+03
R61	1.40	46	0.512	147	1.4E+18	2.0E+17	1.4E+04	7.0E+03
R57	1.61	50	0.457	134			1.9E+04	7.4E+03
R48	1.32	50	0.487	107	1.1E+18	4.6E+17	2.1E+04	7.8E+03
R20	0.98	65	0.448	136	1.4E+18	2.3E+17	1.8E.+04	8.4E+03
R0	0.84	80	0,459	128	7.2E+16	1.1E+17	1.7E+04	8.8E+03
Blank	1.27	74	0.149[b]	740[b]			2.0E+04	2.9E+03

[a] Initial slope r_0 is the tangent to the curve of the EPR signal intensity of spin-trapped $OH^\bullet$ adduct vs. reaction time.

[b] Value extrapolated according to Eq (9).

When the oxidation was by H_2O_2, rutile is more efficient

When it was by O_2, anatase is more efficient due to higher surface area and superoxide trap

The photogenerated charges are very similar to those of pure rutile samples whatever the amount of anatase, showing that e^- and h+ are preferentially trapped on theTi^{3+} and O^{2-}centers of rutile phase, even if anatase is the main component. This indicates that an electron transfer occurs from the higher energy conduction band states of anatase to those of rutile, as lying at lower energy and, simultaneously, a hole transfer occurs from the lower energy valence band states of anatase to those of rutile as lying at higher energy.

Detection of the OH• radicals produced by TiO_2 irradiation

Irradiation has been carried out in the presence of a-(4-pyridyl-1-oxide)-N-tert-butylnitrone (POBN). The following reaction takes place

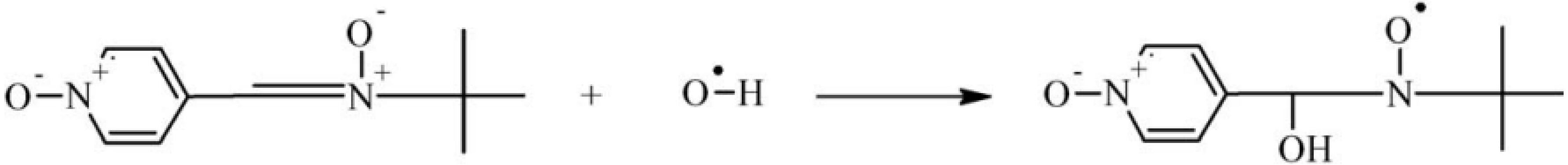

and gives rise to the paramagnetic nitroxyradical.
The amount of OH• is in agreement with the efficacy in the phenol oxidation.

Spectroscopic details

502 *R. Scotti et al. / Applied Catalysis B: Environmental 88 (2009) 497–504*

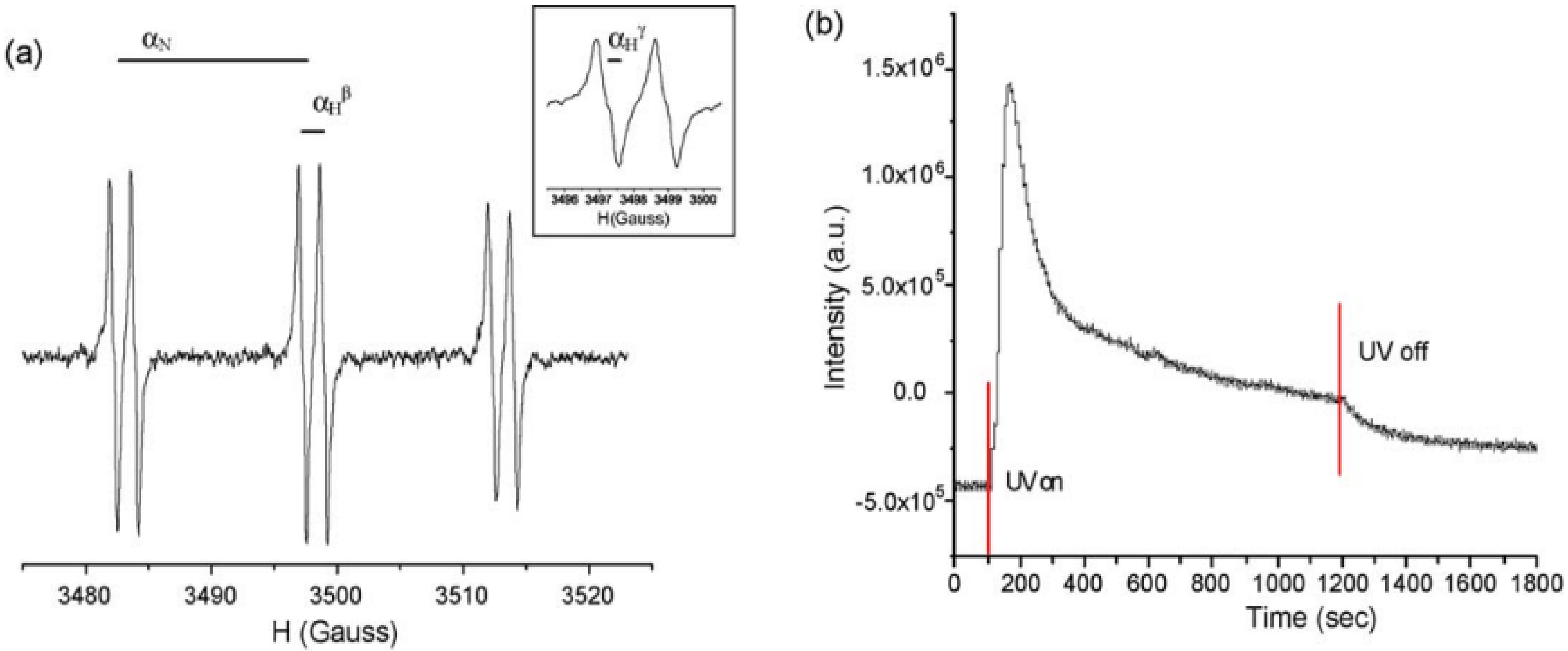

Fig. 4. (a) EPR spectrum of the •POBN-OH adduct. Hyperfine constants a_N, a_H^{β} and, in the inset, a_H^{γ} are indicated. (b) Typical variation of the intensity of •POBN-OH resonance lines with the irradiation time.

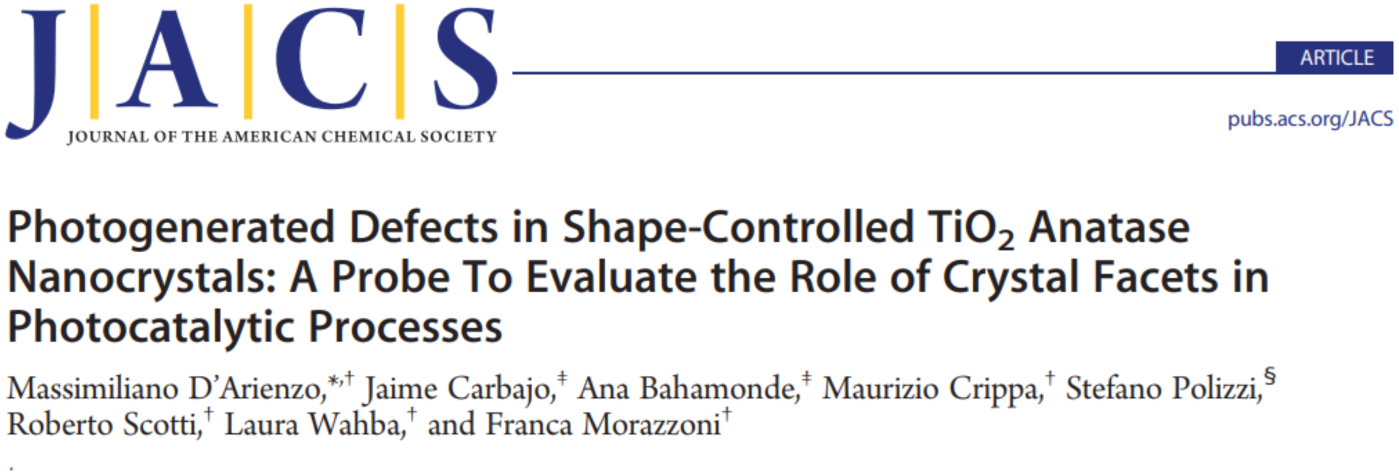

J|A|C|S

JOURNAL OF THE AMERICAN CHEMICAL SOCIETY

ARTICLE

pubs.acs.org/JACS

Photogenerated Defects in Shape-Controlled TiO_2 Anatase Nanocrystals: A Probe To Evaluate the Role of Crystal Facets in Photocatalytic Processes

Massimiliano D'Arienzo,*[†] Jaime Carbajo,[‡] Ana Bahamonde,[‡] Maurizio Crippa,[†] Stefano Polizzi,[§] Roberto Scotti,[†] Laura Wahba,[†] and Franca Morazzoni[†]

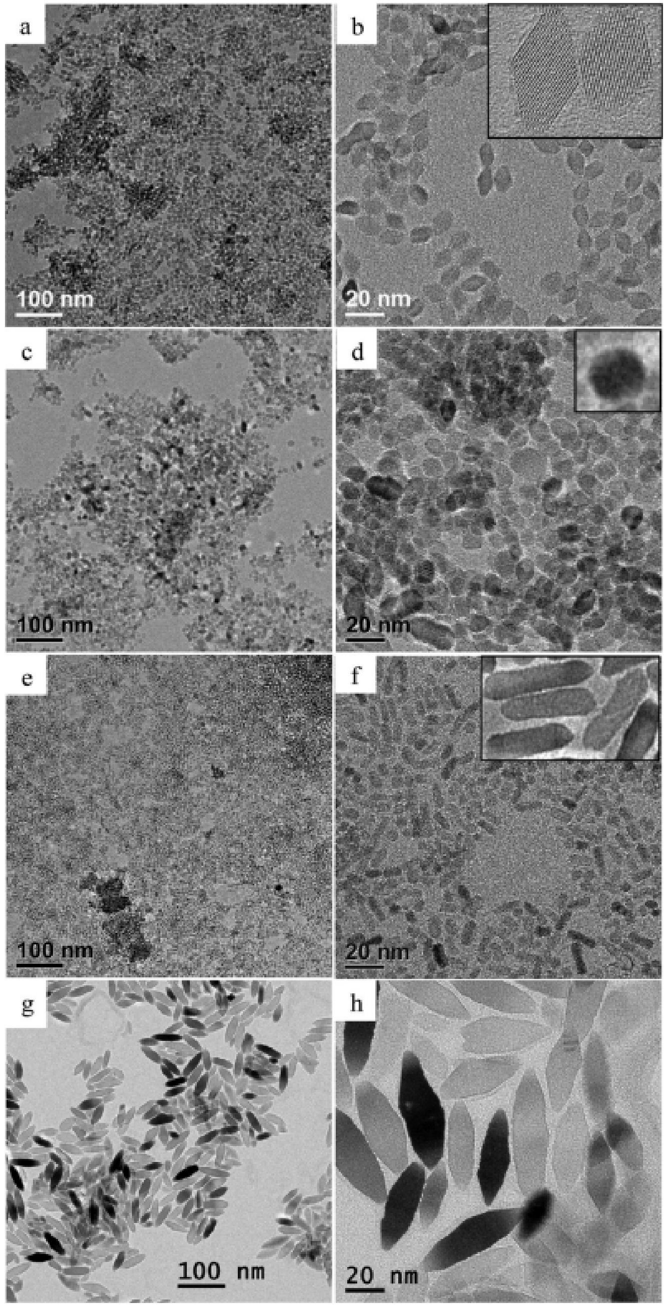

TEM images of the shape-controlled anatase samples: (a,b) R, (c,d) SP, (e,f) NB, and (g,h) RE. Insets in panels b, d, and f are high magnification images of the corresponding shapes

R = rhombic **SP** = spherical **NB** = nanobar **RE =** rhombic elongated

The differences in morphology have as a consequence the difference in the area facets

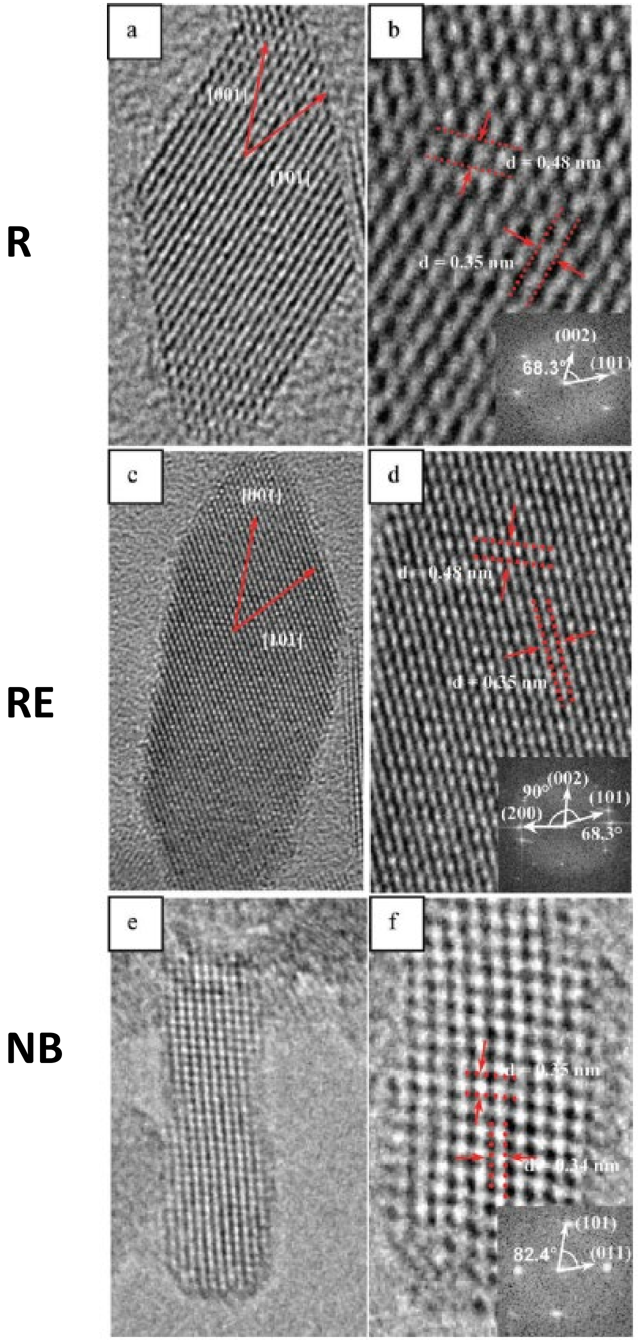

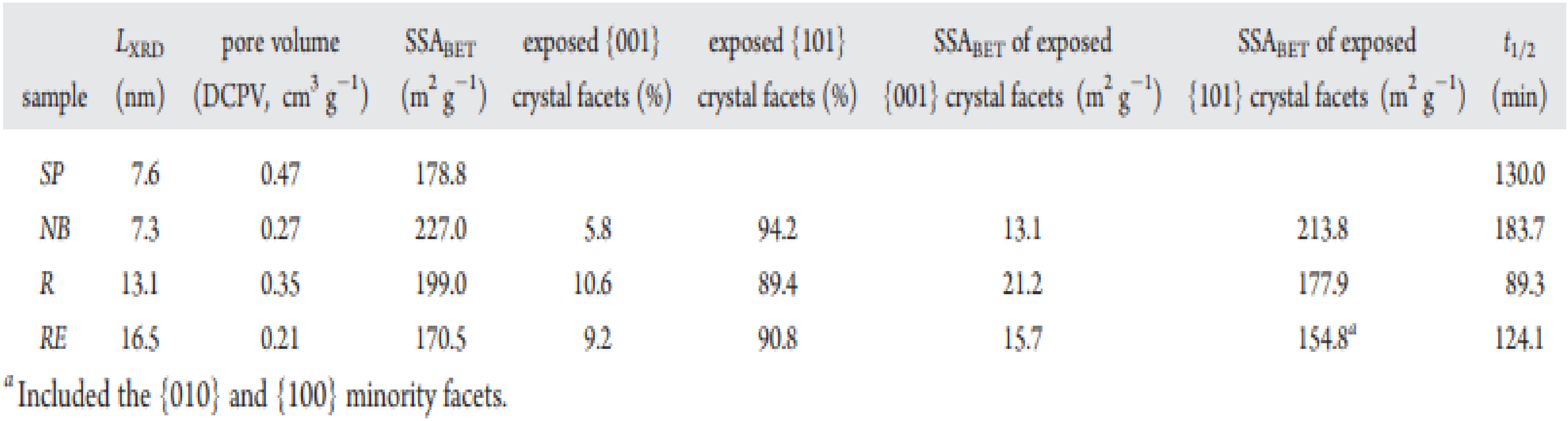

sample	L_{XRD} (nm)	pore volume (DCPV, $cm^3 g^{-1}$)	SSA_{BET} ($m^2 g^{-1}$)	exposed {001} crystal facets (%)	exposed {101} crystal facets (%)	SSA_{BET} of exposed {001} crystal facets ($m^2 g^{-1}$)	SSA_{BET} of exposed {101} crystal facets ($m^2 g^{-1}$)	$t_{1/2}$ (min)
SP	7.6	0.47	178.8					130.0
NB	7.3	0.27	227.0	5.8	94.2	13.1	213.8	183.7
R	13.1	0.35	199.0	10.6	89.4	21.2	177.9	89.3
RE	16.5	0.21	170.5	9.2	90.8	15.7	154.8[a]	124.1

[a] Included the {010} and {100} minority facets.

In rhombic R and rhombic elongated RE particles the Specific Surface Area (SSA) of exposed 001 and 101 facets are higher with respect to the other ones

Pore volume and surface area are lower

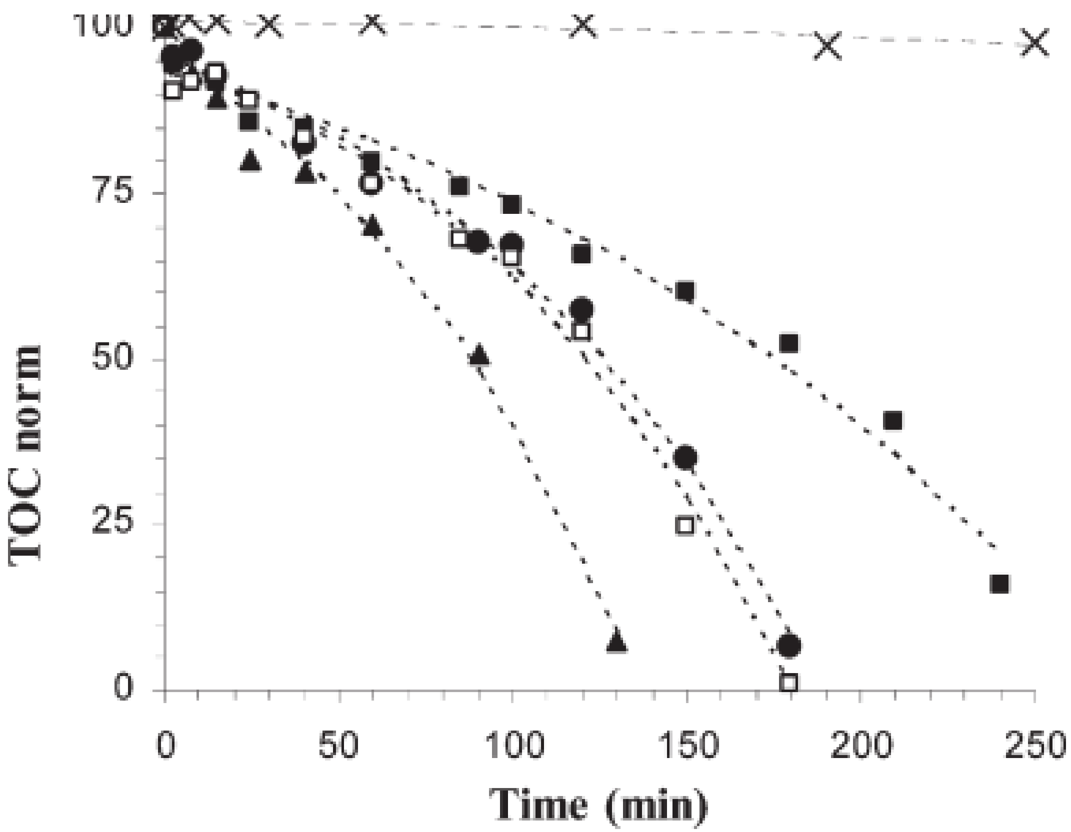

Mineralization curves of phenol (given as TOC%) under UV irradiation in the presence of O2 of (**X**) Blank without catalyst, (■) NB, (●) SP, (□) RE, and R (▲) TiO2 nanocrystals

The catalytic efficacy is depending on the area of the exposed 001 and 101 facets

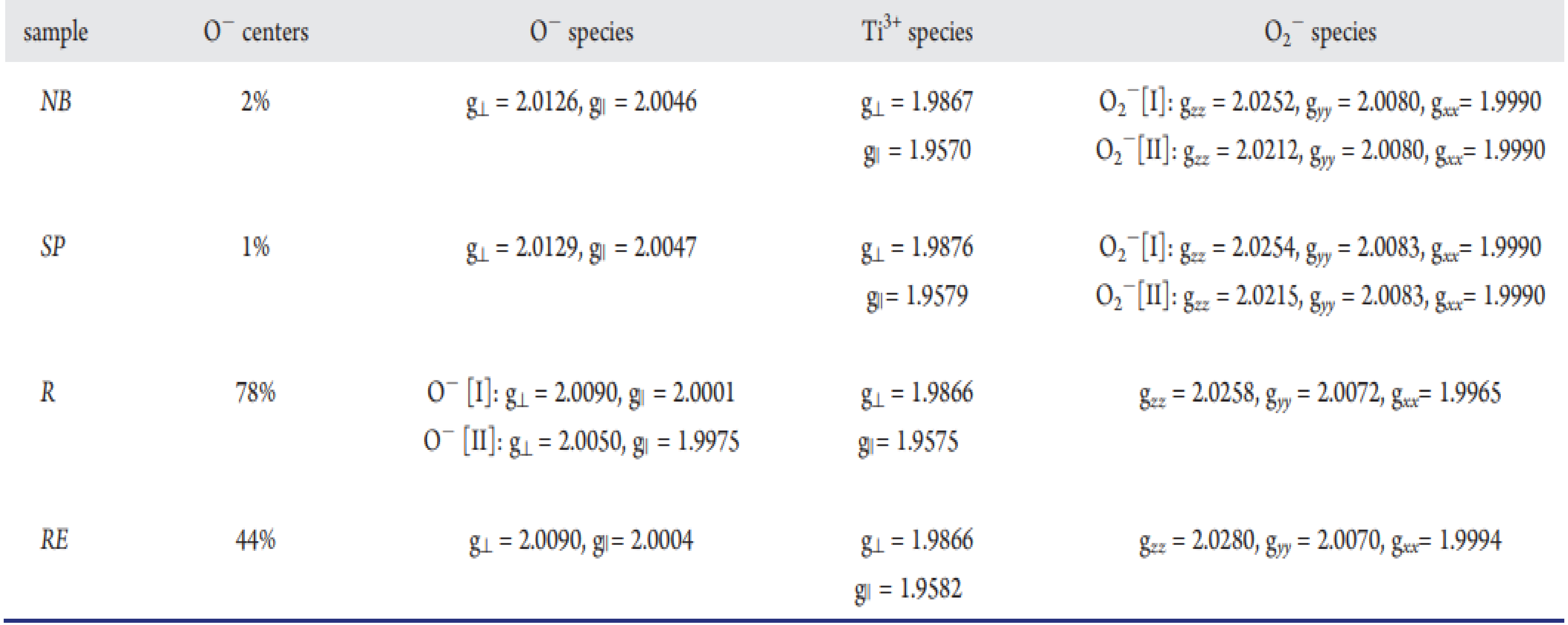

sample	O^- centers	O^- species	Ti^{3+} species	O_2^- species
NB	2%	$g_\perp = 2.0126$, $g_\parallel = 2.0046$	$g_\perp = 1.9867$ $g_\parallel = 1.9570$	O_2^-[I]: $g_{zz} = 2.0252$, $g_{yy} = 2.0080$, $g_{xx} = 1.9990$ O_2^-[II]: $g_{zz} = 2.0212$, $g_{yy} = 2.0080$, $g_{xx} = 1.9990$
SP	1%	$g_\perp = 2.0129$, $g_\parallel = 2.0047$	$g_\perp = 1.9876$ $g_\parallel = 1.9579$	O_2^-[I]: $g_{zz} = 2.0254$, $g_{yy} = 2.0083$, $g_{xx} = 1.9990$ O_2^-[II]: $g_{zz} = 2.0215$, $g_{yy} = 2.0083$, $g_{xx} = 1.9990$
R	78%	O^- [I]: $g_\perp = 2.0090$, $g_\parallel = 2.0001$ O^- [II]: $g_\perp = 2.0050$, $g_\parallel = 1.9975$	$g_\perp = 1.9866$ $g_\parallel = 1.9575$	$g_{zz} = 2.0258$, $g_{yy} = 2.0072$, $g_{xx} = 1.9965$
RE	44%	$g_\perp = 2.0090$, $g_\parallel = 2.0004$	$g_\perp = 1.9866$ $g_\parallel = 1.9582$	$g_{zz} = 2.0280$, $g_{yy} = 2.0070$, $g_{xx} = 1.9994$

Paramagnetic ESR active species for the different TiO_2 particles

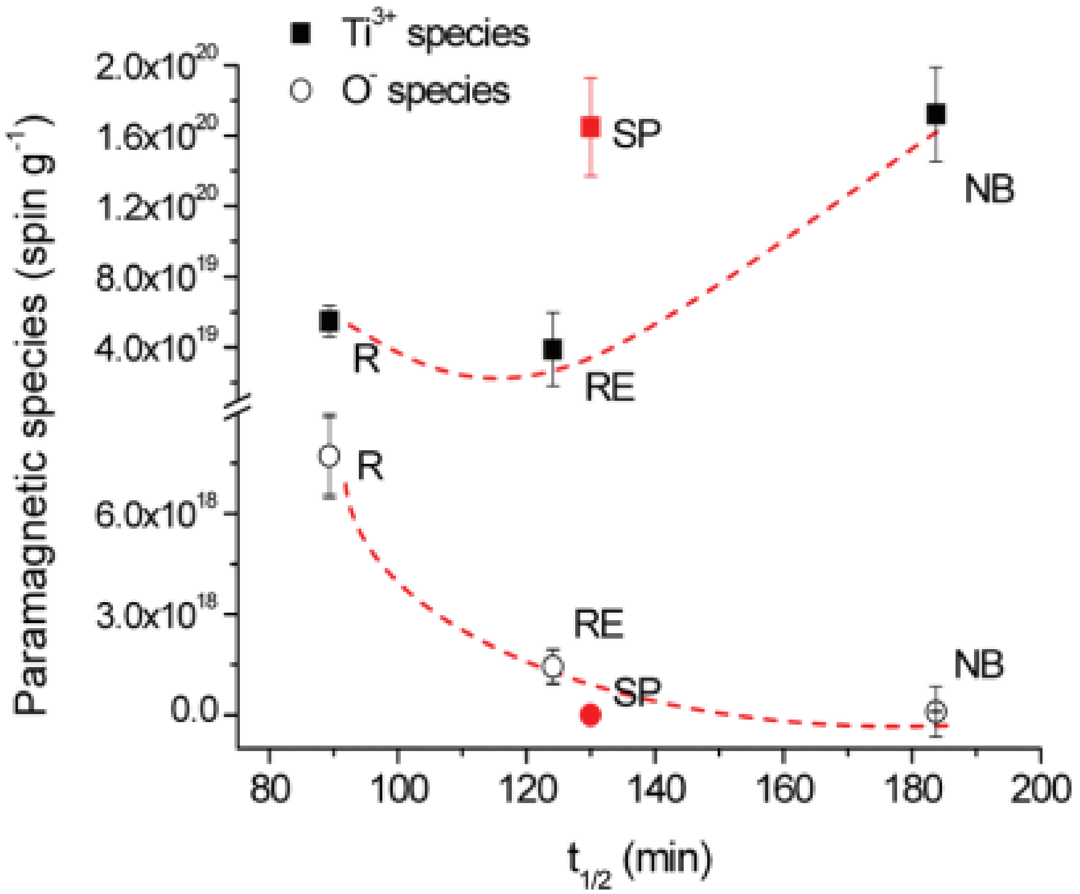

The amount of Ti^{3+} increases increasing the $t_{1/2}$ of the oxidative process

The amount of O^- decreases increasing the $t_{1/2}$ of the oxidative process

These trends clearly suggest a parallel between the photo activity of faceted nanocrystals and the amount of trapped holes, which ultimately drives the surface photooxidation processes.

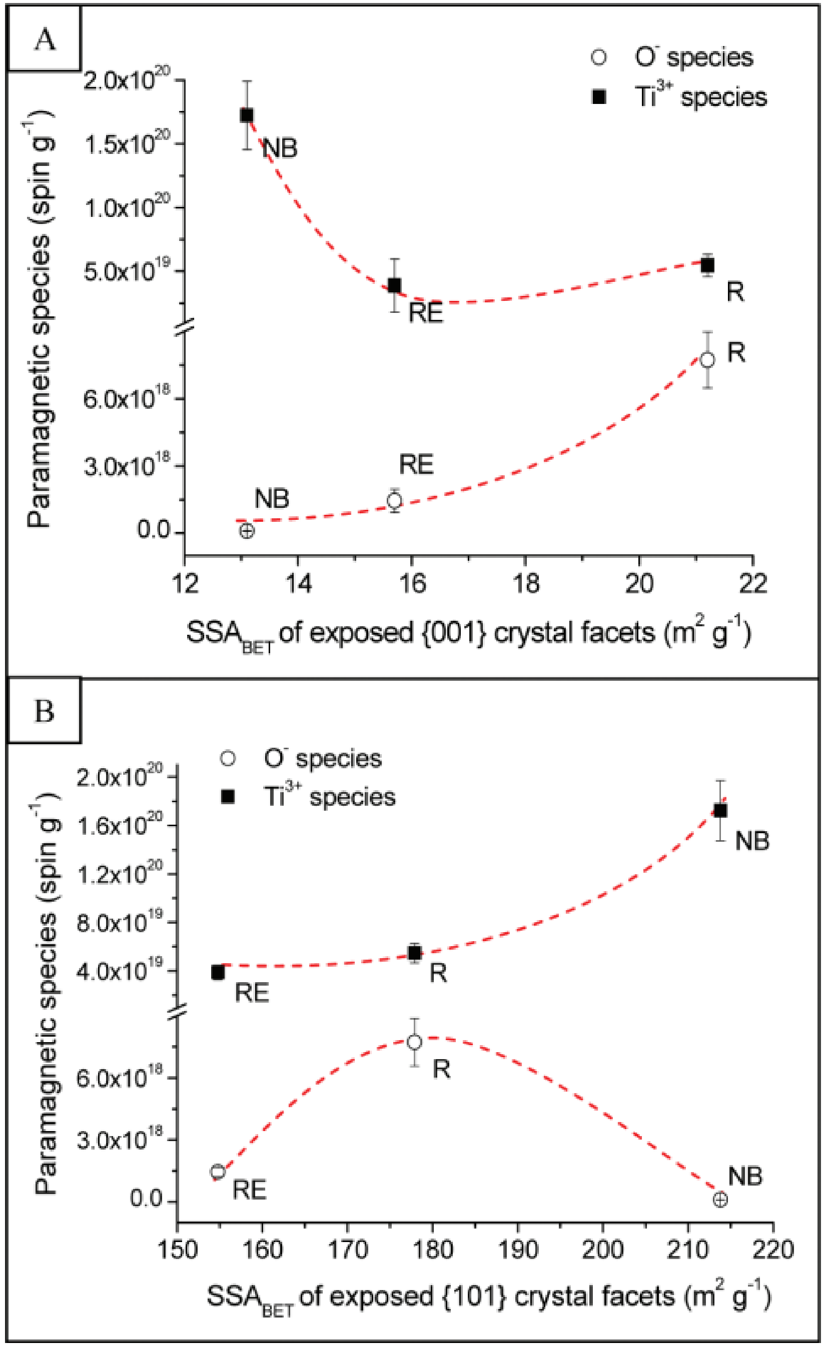

The 001 facets promote the formation of O^-, thus of the oxidation

The 101 facets hinder the formation of O^-, thus they promote the reduction

For this reason the control of the crystal morphology allows to control the catalytic process

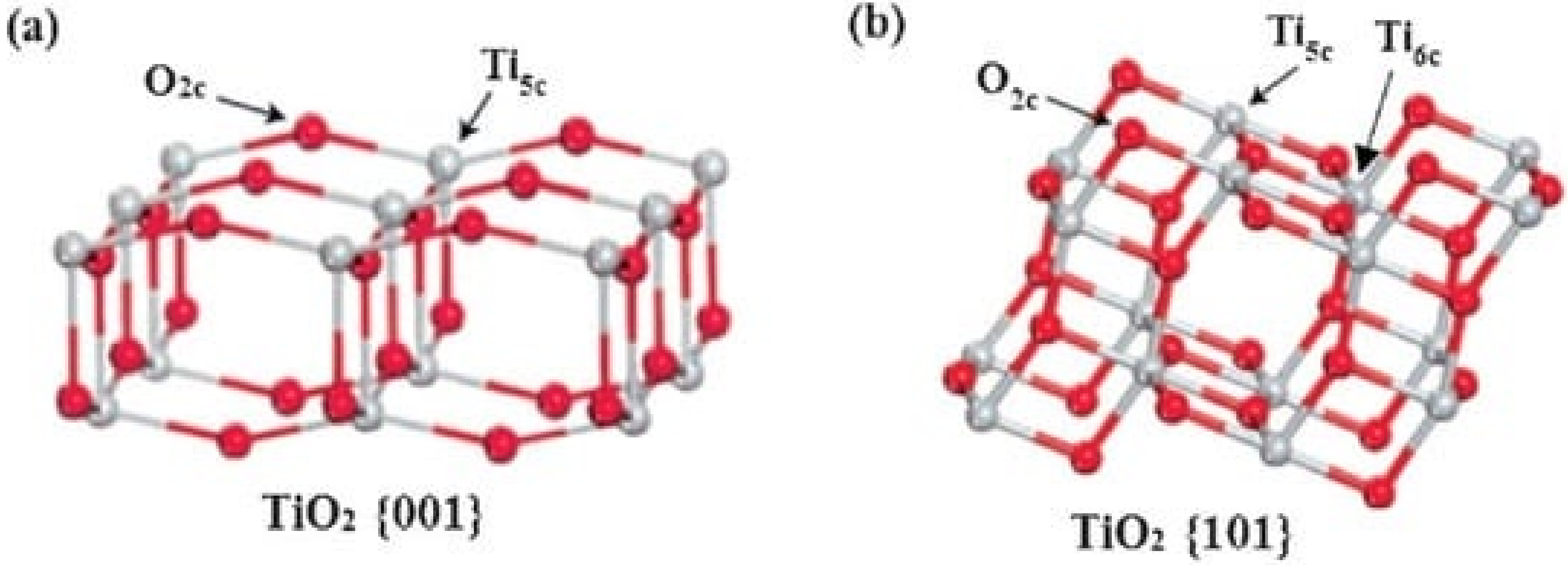

TiO_2 {001}

TiO_2 {101}

Ti^{4+} centers pentacordinated easly accept electrons and induce the formation of holes

J. Phys. Chem. C **2010,** *114,* 15755–15762 **15755**

Membrane-Assisted Charge Separation and Photocatalytic Activity in Embedded TiO_2: A Kinetic and Mechanistic Study

Massimiliano D'Arienzo,* Maurizio Crippa, Amr A. Essawy, Roberto Scotti, Laura Wahba,
and Franca Morazzoni
Department of Materials Science, University of Milano Bicocca, via R. Cozzi 53, I-20125 Milan, Italy

Paolo Gentile
Department of Geological Sciences and Geotechnologies, University of Milano Bicocca, Piazza della Scienza 4, I-20126 Milan, Italy

Ignazio Renato Bellobono
R&D Group, BIT srl, via Pontaccio 14, I-20121, Milan, Italy

TiO2 dispersed in polyester acrylate membranes was tested as a photocatalyst in the phenol mineralization reaction assisted by molecular oxygen. Kinetics experiments revealed that, although embedded, the oxide maintains significant catalytic activity.

The investigation of the photogenerated charge carriers in the photocatalyst demonstrated that **electrons are trapped on Ti^{3+} centers**, while **holes are trapped on C-centered species of the** polymer matrix. In the presence of O2, the C-centered **radicals on the polymer transform into peroxy radicals**, reinforcing the charge separation in the polymer-embedded oxide with respect to the powder.

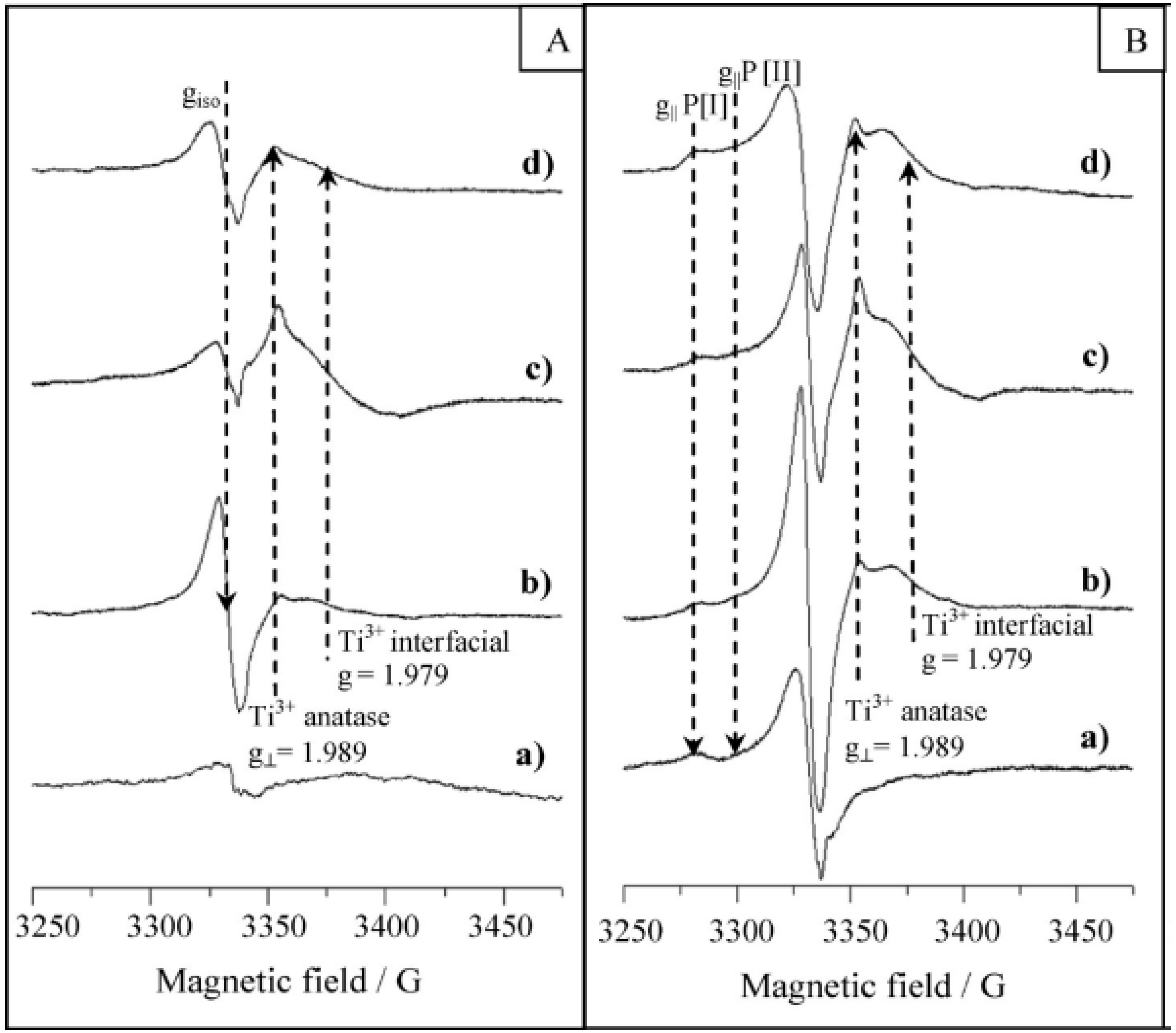

A) ESR spectra under vacuum B) ESR spectra under 7 mbar of O_2

THE JOURNAL OF
PHYSICAL CHEMISTRY C

Article

pubs.acs.org/JPCC

Crystal Surfaces and Fate of Photogenerated Defects in Shape-Controlled Anatase Nanocrystals: Drawing Useful Relations to Improve the H_2 Yield in Methanol Photosteam Reforming

Massimiliano D'Arienzo,*,[†] Maria Vittoria Dozzi,*,[‡] Matteo Redaelli,[†] Barbara Di Credico,[†] Franca Morazzoni,[†] Roberto Scotti,[†] and Stefano Polizzi[§]

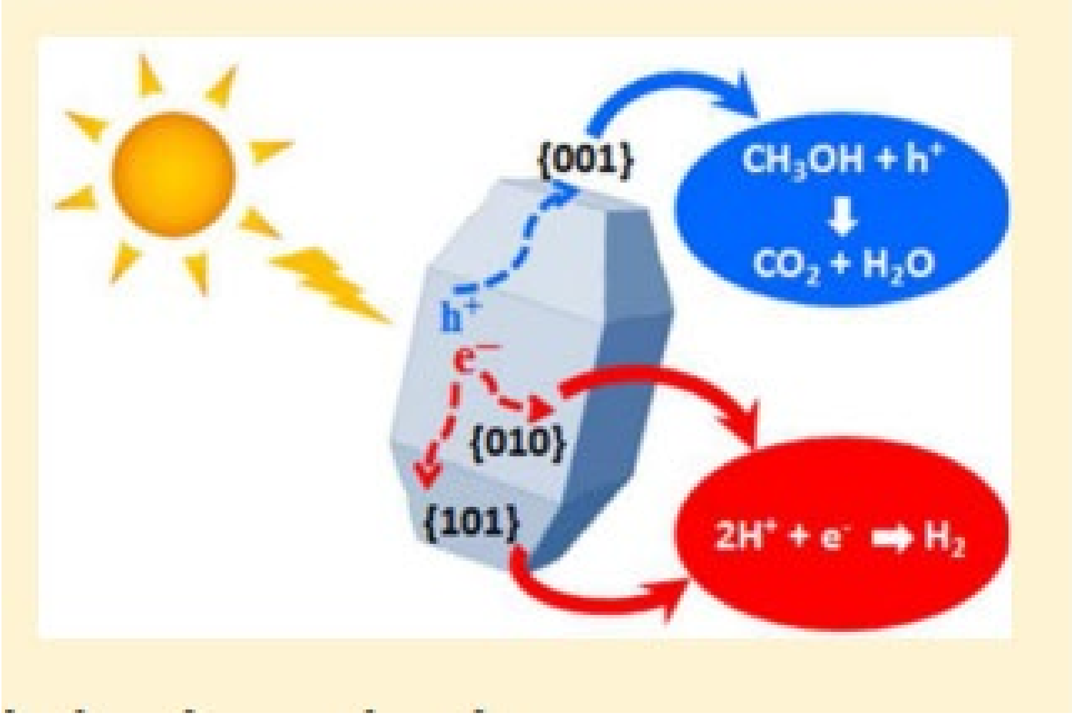

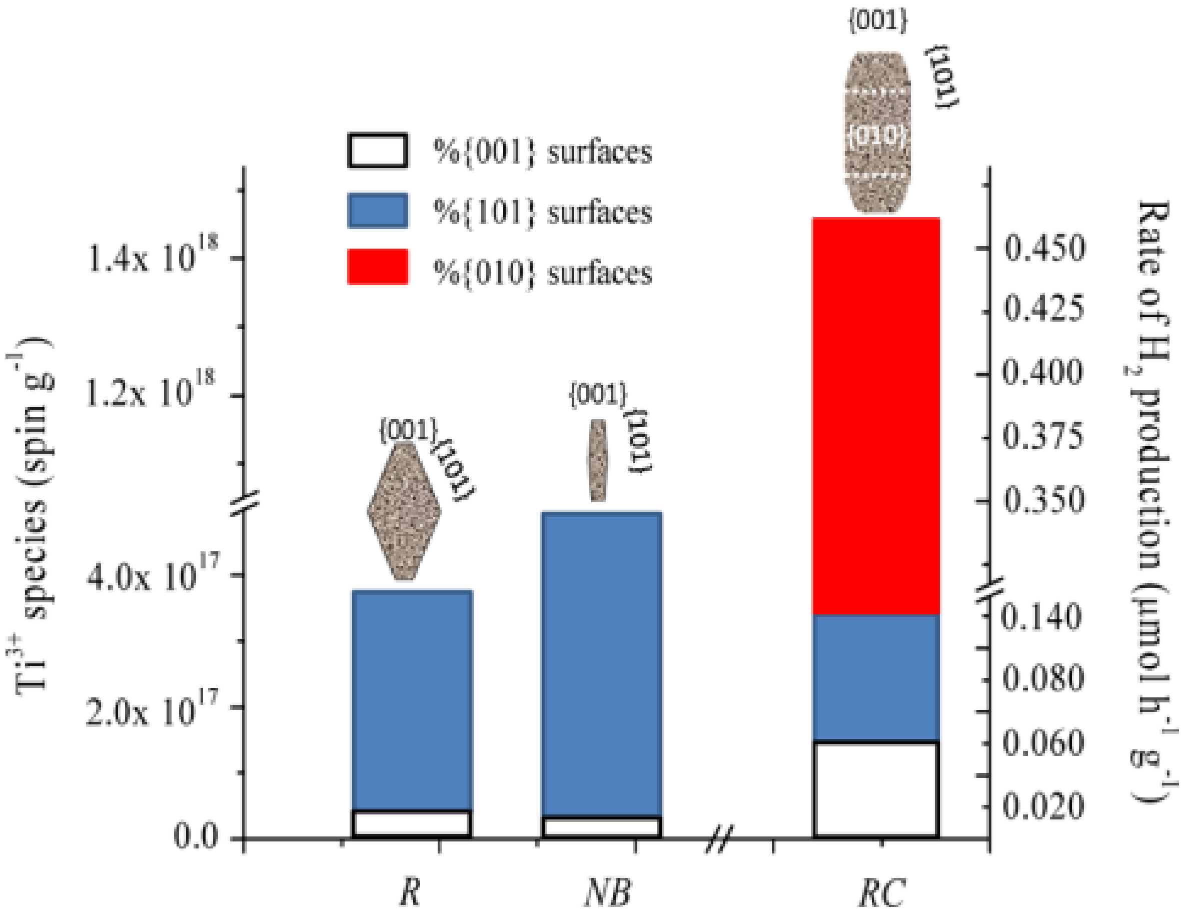

Figure 7. Relative abundance of Ti^{3+} species and measured H$_2$ evolution rate with *RC*, *NB*, and *R* TiO$_2$ nanocrystals as a function of the relative percentage of exposed facets.

R rectangular   R rhombic   NB nanobar

It can be concluded that

The morphology of the catalyst nanoparticles allows to control their photocatalytic activity

Within the same morphology, the structure of the exposed facets can induce different reactivity

The ability of ESR to investigate the symmetry of the reacted sites elucidates the catalytic mechanism and allows its optimization

Grazie Renato della tua guida! Buon Compleanno!

Franca Morazzoni
Barbara Di Credico
Massimiliano D’Arienzo
Roberto Scotti